IOP PUBLISHING JOURNAL OF PHYSICS D: APPLIED PHYSICS

J. Phys. D: Appl. Phys. **42** (2009) 175409 (10pp) doi:10.1088/0022-3727/42/17/175409

A computational study on the effective properties of heterogeneous random media containing particulate inclusions

Elyas Tawerghi and Yun-Bo Yi

Department of Mechanical and Materials Engineering, University of Denver, Denver, CO 80208, USA

E-mail: yyi2@du.edu

Received 31 December 2008, in final form 16 July 2009
Published 12 August 2009
Online at stacks.iop.org/JPhysD/42/175409

Abstract

The effective elastic modulus and conductivity of a two-phase material system are investigated computationally using a Monte Carlo scheme. The models contain circular, spherical or ellipsoidal inclusions that are either uniformly or randomly embedded in the matrix material. The computed results are compared with the applicable effective medium theories. It is found that the random distribution, geometric permeability and particle aspect ratio have non-negligible effects on the effective material properties. For spherical inclusions, the effective medium approximations agree well with the simulation results in general, but the analytical predictions on void or non-spherical inclusions are much less reliable. It is found that the results for overlapping and non-overlapping inclusions do not differ very much at the same volume fraction. The effect of particle morphology is also investigated by modelling prolate and oblate ellipsoidal inclusions.

(Some figures in this article are in colour only in the electronic version)

1. Introduction

Over the last few decades there has been a recurrent interest in predicting the effective material properties of advanced heterogeneous composites [1, 2]. The main interest has been focused on the maximum achievable elastic modulus and conductivity, using either analytical or numerical approaches [3, 4]. A number of mechanical, physical and mathematical principles were employed to derive approximate solutions for estimating the effective properties of multiphase material systems.

Prediction of the percolation threshold is usually a first step. For example, Yi and Sastry [5] derived analytic approximations for percolation points in two-dimensional (2D) and three-dimensional (3D) ellipsoids based on the series expansion method. Yi [6] also studied the void percolation problem of a medium containing overlapping ellipsoids. These results are useful in predicting the minimum amount of material needed to achieve conduction or mechanical strength. In addition to the predictions of the percolation threshold, the elastic modulus and conductivity of fibrous networks [7, 8] or particulate systems [9] were also studied computationally. However, these works were based on the single-phase system in which the fibres or particles are the only material phase. More realistic composite systems consist of at least two phases: the matrix materials, which are used for structural integrity, and fillers, which are used for improving mechanical, thermal or electrical performance. In modelling a multiphase material system, the physical connections between different material phases must be taken into careful consideration.

It is well known that the effective medium theories (EMTs) can be used to estimate the effective properties of multiphase materials for a wide range of volume fractions [1, 10]. Examples of these theories include the linear rules of mixing [11], the Maxwell approximation [12], the self-consistent approximation [13] and the differential effective medium theory [14]. For example, Mondescu and Muthukumar [15] derived closed form solutions for randomly disturbed particles at low volume fraction based on the EMTs.

However, there is always an uncertainty associated with the numerical accuracy of EMTs [16]. Therefore, in addition to analytical approaches, computational methods have been widely used to investigate the problem, and perhaps the most widespread method is the derived finite element analysis

using digital images for composite materials [3, 17]. This method requires a particular error analysis in deriving the results. An application of this method was explored by Roberts and Garboczi who studied linear elastic properties of random porous composites with various microstructures [18]. However, reduction in local maximum errors, particularly at material boundaries, is not guaranteed. In an alternative approach there is no need to take x-ray of composite materials to obtain digitalized images for finite element analysis. This approach is based on various state-of-the-art software packages to analyse the morphology and properties of composite structures. For example, Cai applied this concept to compute the thermal conductivity of PTEE composite [19].

Dealing with the finite element modelling of a multiphase material system is by no means an easy task, since the inclusion materials are interconnected with the matrix. The persistent obstacles to mesh automation of complex structures are well known and no individual commercial code is capable of handling the problem of interest. In this work, we employ a new, direct simulation method that does not rely on digitization of the material phase, thus allowing more accurate modelling of the interconnected structures. The method is based on the direct Delaunay tessellation scheme, i.e. a general triangulation method from scattered points. Several commercial codes worked jointly in the model development: Matlab® [20], Comsol Multiphysics® [21] and Abaqus® [22], as well as a standalone code written in C programming language for particle dispersion. The analytical approximations have also been obtained from the EMTs, for both validation and comparison purposes.

For realistic multiphase composites, the interfacial effect could play an important role. For example, Torquato and Rintoul [23] developed rigorous bounds on effective conductivity for the interfacial surface effect between spherical inclusions and matrix, and this work was later extended for other problems as well [24, 25]. In addition, the mechanical contact problems were investigated in the context of random media recently [26]. This work, however, is focused on the morphological effects on the properties, and the interfacial effects have therefore been ignored for computational efficiency. The methodology itself, however, can in principle be applied to a more general situation incorporating interfacial effects as well.

2. Methods

2.1. Effective medium approximations

Equations (1)–(3) define the Maxwell approximation scheme for the effective elastic modulus and conductivity of d-dimensional systems ($d = 2$ for 2D systems and $d = 3$ for 3D systems) containing spherical inclusions. For circular void inclusions, equation (4) was used to obtain the analytical solutions, and the matrix in this case was assumed to be incompressible where $K_2/K_1 = \infty$, and the circular voids are cavities where $K_2 = G_2 = 0$. Here K represents the bulk modulus, which is defined by $K = E/[3(1-2\nu)]$, and G is the shear modulus, which is defined by $G = E/[2(1+\nu)]$. In the above definitions, E is the elastic modulus and ν is Poisson's ratio. The subscripts '1' and '2' correspond to the matrix phase and the inclusion phase, respectively.

$$\frac{G_e - G_1}{G_e + H_1} = \phi_2 \left[\frac{G_2 - G_1}{G_2 + H_1}\right], \tag{1}$$

$$H_i \equiv \frac{G_i\,[dK_i/2 + (d+1)\,(d-2)\,G_i/d]}{K_i + 2G_i}, \qquad i = 1, 2, \tag{2}$$

$$\frac{\sigma_e - \sigma_1}{\sigma_e + (d-1)\sigma_1} = \phi_2 \left[\frac{\sigma_e - \sigma_1}{\sigma_2 + (d-1)\sigma_1}\right], \tag{3}$$

$$\frac{G_e}{G_1} = \frac{d(1-\phi_2)}{d - 2\phi_2}, \qquad K_2 = G_2 = 0, \qquad \frac{K_1}{G_1} = \infty. \tag{4}$$

In these equations, ϕ_2 is the volume fraction of the inclusions (the volume fraction of the matrix, ϕ_1, is thus equal to $1-\phi_2$); G_1, G_2 and G_e are the shear modulus of the matrix, the shear modulus of the inclusions and the overall effective shear modulus, respectively; σ_1, σ_2 and σ_e are the conductivity of the matrix, the conductivity of the inclusions and the overall effective conductivity, respectively.

The explicit formulae of the self-consistent (SC) approximation are shown in equations (5)–(9). Equation (10) is the form of the SC approximation for void inclusions, and the matrix is again assumed to be incompressible here.

$$\sum_{j=1}^{M} \phi_2 \frac{G_j - G_e}{G_j + H_e} = 0, \tag{5}$$

$$H_e \equiv \frac{G_e\,[dK_e/2 + (d+1)(d-1)G_e/d]}{K_e + 2G_e}, \tag{6}$$

$$\sum_{j=1}^{M} \phi_2 \frac{\sigma_j - \sigma_e}{\sigma_j + (d-1)\sigma_e} = 0, \tag{7}$$

$$\sigma_e = \frac{\alpha + \sqrt{\alpha^2 + 4(d-1)\sigma_1\sigma_2}}{2(d-1)}, \tag{8}$$

$$\alpha = \sigma_1(d\phi_1 - 1) + \sigma_2(d\phi_2 - 1), \tag{9}$$

$$\frac{G_e}{G_1} = \frac{d\,[(d-1) - (d+1)\phi_2]}{d(d-1) - 2\phi_2}. \tag{10}$$

In these equations, M represents the number of different types of inclusions.

Finally, the differential effective medium (DEM) approximation is an indirect approximation approach. The implicit formulae for this approach are shown in equations (11) and (12) as follows:

$$(1-\phi_2)\frac{\mathrm{d}G_e}{\mathrm{d}\phi_2} = \left[G_j + H_e\right]\frac{G_2 - G_e}{G_2 + H_e}, \tag{11}$$

$$\left(\frac{\sigma_2 - \sigma_e}{\sigma_2 - \sigma_1}\right)\left(\frac{\sigma_1}{\sigma_e}\right)^{1/d} = 1 - \phi_2. \tag{12}$$

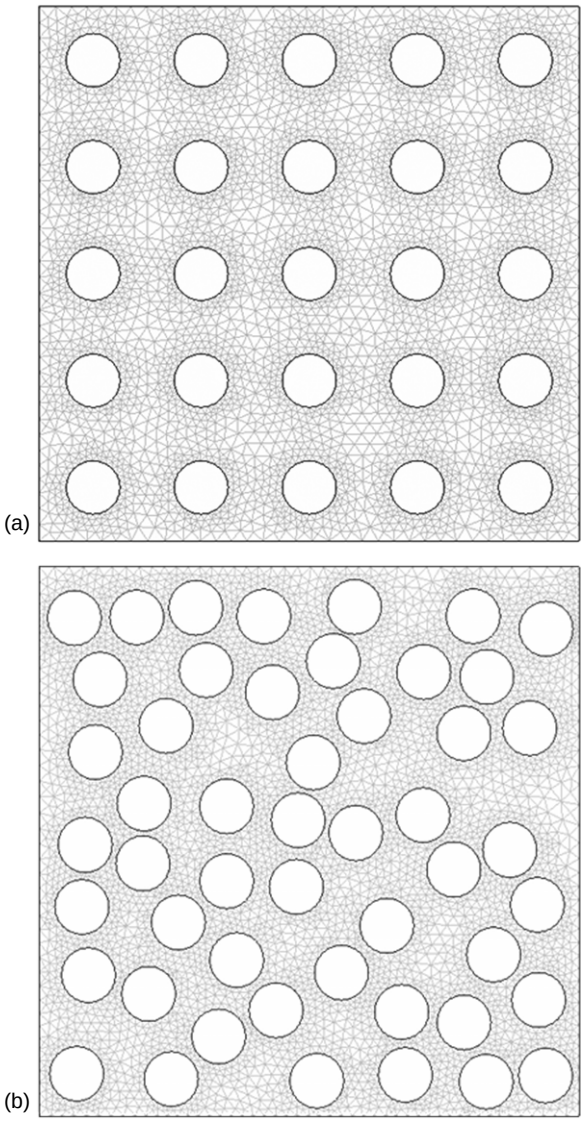

Figure 1. Finite element model of a unit square plate containing (*a*) uniformly distributed circular voids with 19.6% void volume fraction and (*b*) randomly distributed circular voids with 38.5% void volume fraction.

2.2. Two-dimensional computational models

In the 2D simulations, Matlab® and Comsol® were directly used to create finite element models in a rectangular simulation domain of unit size required for the subsequent mechanical analysis. In particular, a dynamic collision algorithm was applied to randomly deploy non-overlapping voids or fillers. The finite element mesh was then generated by using the built-in functions in Comsol® and the analyses were performed via a user friendly interface of the software.

Three different scenarios were studied as follows. Case (1)—arrays of circular voids were uniformly distributed in the domain with the same spacing in both x- and y-directions. The voids had the same size with a fixed radius of 0.05. Optimized mesh quality was achieved for the finite element analysis and figure 1(*a*) shows an example of such a model. The number of triangular elements in the model was 6800 elements. Case (2)—the circular voids were randomly dispersed in the domain. 'Random' here is referred to as a Poisson process following a uniform probability density. Figure 1(*b*) shows an example of randomly distributed circular voids with 7447 elements. Case (3)—the circular voids in case (2) were replaced by disc-shaped circular fillers, and therefore two dissimilar materials were involved in this scenario.

The mechanical boundary was constrained by applying a prescribed displacement of 0.01 along the y-direction, and an isotropic linear elastic analysis was performed to determine the reaction forces. The effective elastic modulus of the system was estimated by taking the ratio of the resulting stress to the preset strain. According to the scaling theories, the result computed in this way is a function of the simulation domain. However, when the ratio of the domain size to the diameter of inclusions is sufficiently large, the result will approach the asymptotic limit. Several physical assumptions and mathematical simplifications were made: (1) for circular fillers, the two phases had the same Poisson's ratio (0.3) to minimize the total number of variables in the model; (2) the interfaces between dissimilar materials were bonded by either adhesives or special chemical or thermal treatment, therefore no contact surfaces were modelled; (3) the simulation results were normalized against the properties of the matrix, and hence the modulus or conductivity is dimensionless.

2.3. Three-dimensional computational models

In the 3D simulations, a different scheme was implemented to automate the modelling process, due to the difficulties in a direct simulation using the existing commercial codes. It involved a three-step procedure: first, a similar collision algorithm was employed to generate overlapping or non-overlapping inclusions. Second, the obtained geometric data were used to generate a finite element mesh by a standard Delaunay tessellation scheme. In the last step, the output data of the code bundle was written into a script file readable by ABAQUS® for the subsequent finite element analysis.

Three different models were investigated: (1) overlapping spherical inclusions, (2) non-overlapping spherical inclusions and (3) non-overlapping ellipsoidal inclusions. Since the problem involving void inclusions were already studied in the 2D cases, here our attention was focused on the continuum problems and the inclusions in all three models were assumed to be fillers.

In the first model, all the spheres were identical and had a radius of 0.1 (the simulation domain remains as a unit cell). These spheres were deployed randomly in the matrix following an algorithm similar to the one used in the 2D models. The tetrahedron finite element mesh was generated via a 3D Delaunay tessellation scheme in Matlab®. The volume fraction of spheres was obtained by summing the volume of each individual element that was located in the interior of at least one sphere. Figures 2(*a*) and (*b*) show the pictures of the mid-plane cross sections of overlapping spheres. In the final step, the mesh data were exported to an ABAQUS® input file. In addition to mechanical analysis,

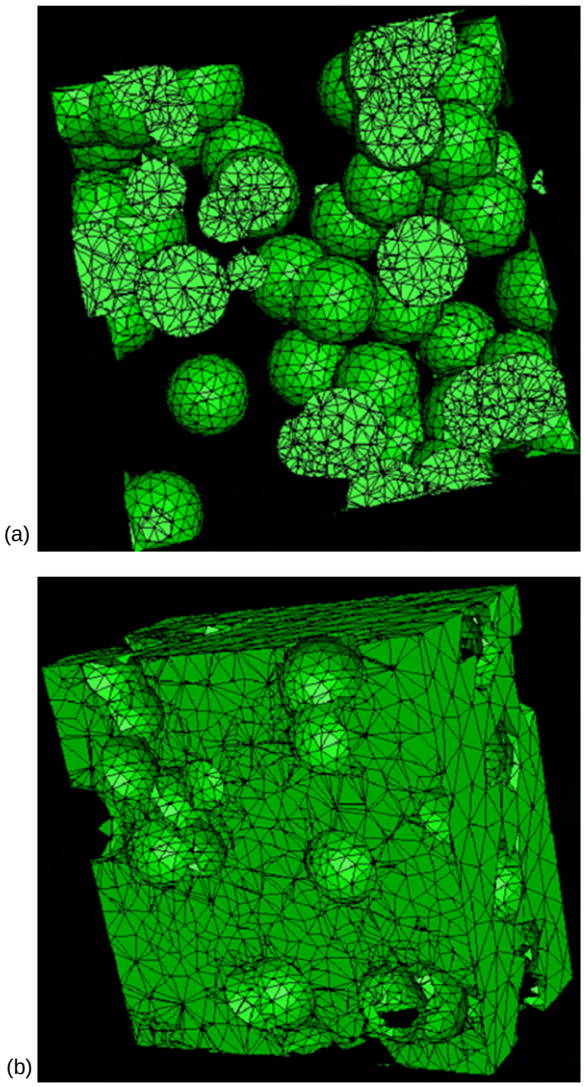

Figure 2. 3D finite element model in a unit cubical domain for (*a*) overlapping spherical particles and (*b*) cross section along the mid-plane of the matrix with spheres removed.

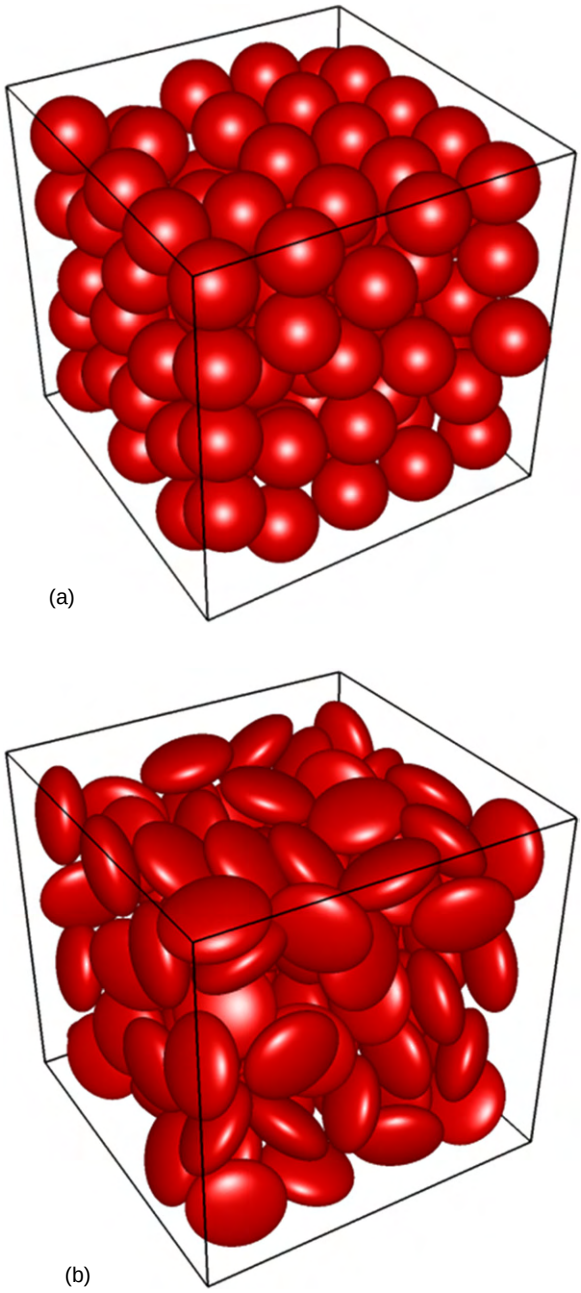

Figure 3. Computer-generated models of (*a*) non-overlapping spheres, and (*b*) non-overlapping ellipsoids.

the effective conductivity of the material system was also evaluated by a steady state heat transfer analysis. More specifically, unit temperature difference was applied on two opposite sides of the unit cell and the reactive heat flux was computed. The total heat transfer rate by summing the nodal heat flux is equivalent to the effective conductivity of the system. Regardless of the physical distinction between thermal and electrical conductions, the normalized result can be interpreted as either the thermal conductivity or electrical conductivity because of the mathematical analogy between the two phenomena.

Non-overlapping spheres were modelled in a strategy similar to that for circular discs, except that the process was more computationally intensive. Figure 3(*a*) shows a computer-generated system of non-overlapping random spheres.

In addition to spherical inclusions, we developed a model for simulating ellipsoidal inclusions. Two types of ellipsoidal particles, oblate (disc-shaped) and prolate (cigar-shaped) were modelled and investigated. Figure 3(*b*) shows a computer-generated random system of oblate ellipsoidal particles. All the ellipsoids were assumed impermeable. The locations and geometric data of ellipsoidal particles were generated in the same way as that used for spherical particles. Although a generalized ellipsoid would be a tri-axial particle, here we focused on ellipsoids of revolution only. Therefore only two parameters were sufficient to determine the geometric shape of each particle: namely, minor axis length and major axis length. To generate random ellipsoidal particles, not only are the centrepoint locations distributed randomly but also the Euler angles of the axes must follow the appropriate density functions of probability.

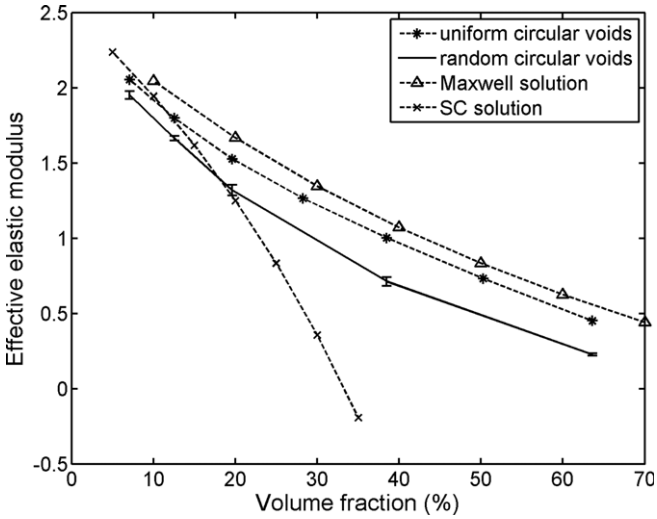

Figure 4. Comparison of normalized elastic modulus between simulations and effective medium approximations for both uniform and random circular void models.

3. Results

3.1. Circular inclusions

We first investigated the effect of circular voids on the elastic modulus. Figure 4 shows a plot of the simulated elastic modulus obtained from the finite element analysis in the following two cases: (1) uniformly distributed circular voids and (2) randomly distributed circular voids. It can be seen that the effective elastic modulus decreases with the void volume fraction in both cases. In addition, the modulus of the material containing uniformly distributed circular voids is higher than that of the material containing randomly distributed voids. The reason could be the effect of the higher stress concentration in the regions where the voids are located very close to each other in the second case. In the same figure, the simulation result is also compared with the EMTs including the Maxwell approximation and the SC approximation. Even though the assumption here is that the matrix is assumed to be incompressible, the Maxwell approximation shows a similar pattern compared with uniformly distributed voids. The SC approximation also shows agreement with the simulations for both uniform and random distributions at lower volume fractions. However, there is a significant discrepancy at higher volume fractions. Overall, the simulation results roughly fall between the Maxwell approximation and the SC approximation results.

To investigate the effect of a two-phase material system, the void spaces in the previous model were replaced by elastic circular discs in figure 5(*a*), where the results are shown for the effective elastic modulus of a plate containing randomly distributed discs. A comparison has been made between the simulations and those predicted by the linear rules of mixing. In parts (*a*), (*b*) and (*c*) of figure 5, the normalized modulus of the inclusions varies from 2, 5 to 7, respectively, whereas a unit elastic modulus has been maintained for the matrix material. It can be seen that the simulation results fall between the upper and lower limits of the linear rules of mixing [11].

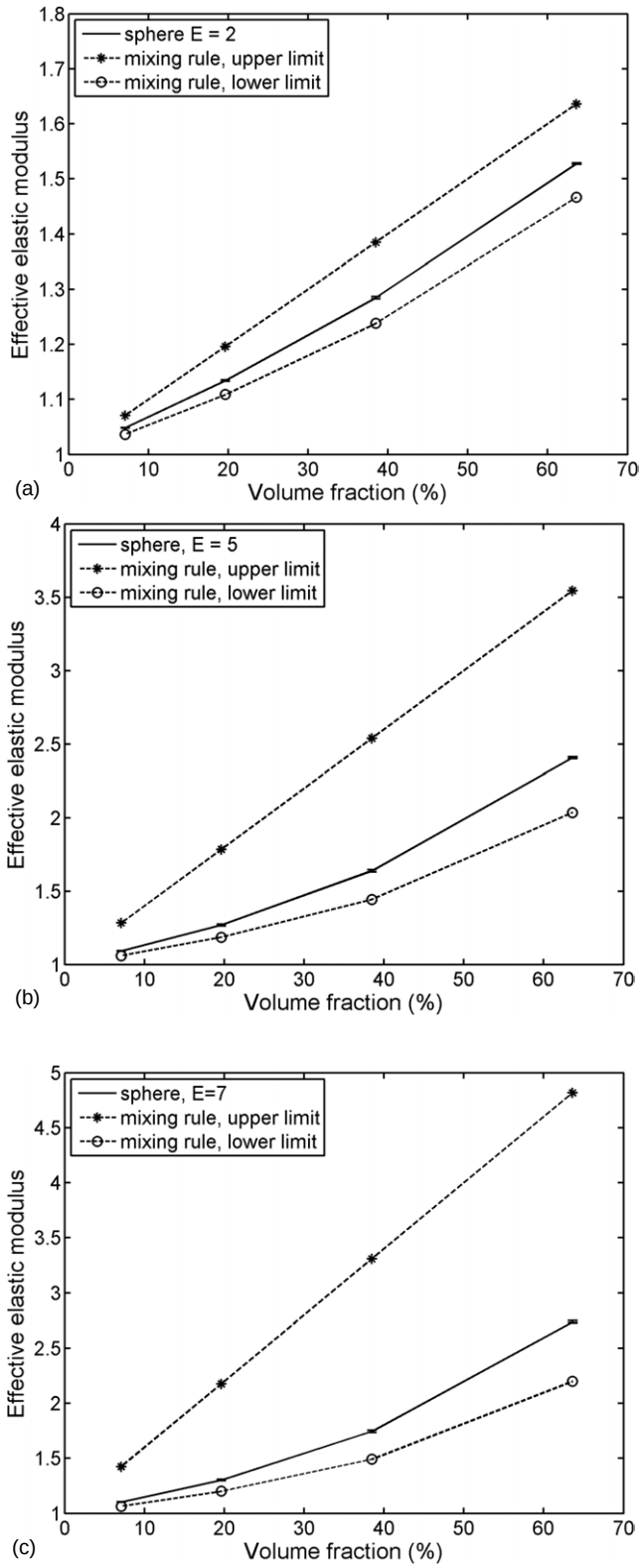

Figure 5. Comparison of normalized elastic modulus between simulations and linear rules of mixing for models containing non-overlapping random circular inclusions, with (*a*) $E_2 = 2$, (*b*) $E_2 = 5$ and (*c*) $E_2 = 7$.

In addition, the difference between the upper and lower limits increases with the modulus of the discs. Apparently, the effective modulus of the composite material increases with both the volume fraction and the modulus of the embedded

particles. For example, the effective moduli (E_{eff}) increase by 40% at 50% volume fraction of discs with $E_2/E_1 = 2$. At the same volume fraction, E_{eff} increases by 100% and 130% for $E_2/E_1 = 5$ and 7, respectively. Similar results have also been obtained for uniformly distributed disc-like inclusions.

Figure 6(*a*) shows the comparison between the finite element simulation and the EMTs. The simulation models along with all the assumptions remain the same as those used in figure 5. It is seen that the effective modulus of the system falls between the Maxwell and the SC approximations. In figure 6(*a*) where $E_2/E_1 = 2$, an excellent agreement is achieved for the entire range of volume fraction. Using either of the approximation theories would yield an error less than 2% in the predicted elastic modulus. In figures 6(*b*) and (*c*) where $E_2/E_1 = 5$ and 7, respectively, the simulation result shows good agreement with the approximation theories at a volume fraction below 40%. At a volume fraction above 40%, the results deviate slightly from the approximation theories. Nevertheless, the Maxwell theory and the SC approximation consistently provide a lower and an upper bound for the simulation results, respectively.

3.2. Spherical inclusions

The above work was extended to the 3D case in which the matrix contains randomly distributed spherical particles instead of circular discs. Figure 7 shows a comparison of the elastic modulus between the simulation and the approximation theories. The spheres are allowed to overlap in this case and $E_2/E_1 = 4$ is assumed. Poisson's ratio is fixed to 0.23 in both phases. It can be seen that the simulation results fall between the Maxwell and the SC approximation theories. Apparently, the effective modulus increases with the sphere volume fraction. Also, it has been noticed that the SC approximation generally yields much better results than the Maxwell approximation.

In addition to the mechanical analysis, we also performed the conductivity analysis for overlapping spheres as shown in figure 8. The dimensionless conductivities of the matrix material and the spherical inclusions are assumed to be 1 and 4, respectively. The simulation results are compared with the three different effective medium solutions: Maxwell, SC and DEM. It is seen that the effective conductivity increases with the sphere volume fraction according to a power-law form similar to the elastic modulus. All the three approximations agree very well at lower volume fractions, especially below 20%. However, differences among FEM, DEM and Maxwell can clearly be seen at higher volume fractions. In comparison with the simulation results, the SC solution once again presents the best solution among the three approximation methods.

The above work was further extended to *non-overlapping* spherical inclusions, which are believed to represent more realistic material systems. The predicted effective elasticity modulus and conductivity are shown in figures 9, 10 and 11. For mechanical analysis, figures 9(*a*), (*b*) and (*c*) show the effective elastic modulus for three cases where $E_2/E_1 = 2$, 4 and 0.25, respectively. In figure 9(*a*), it can be seen that the simulation results are in excellent agreement with the approximation solutions. In figure 9(*b*), the difference is discernable, but not quite significant. At lower volume fractions, the SC solution is closer to the simulation results whereas at higher volume fractions the

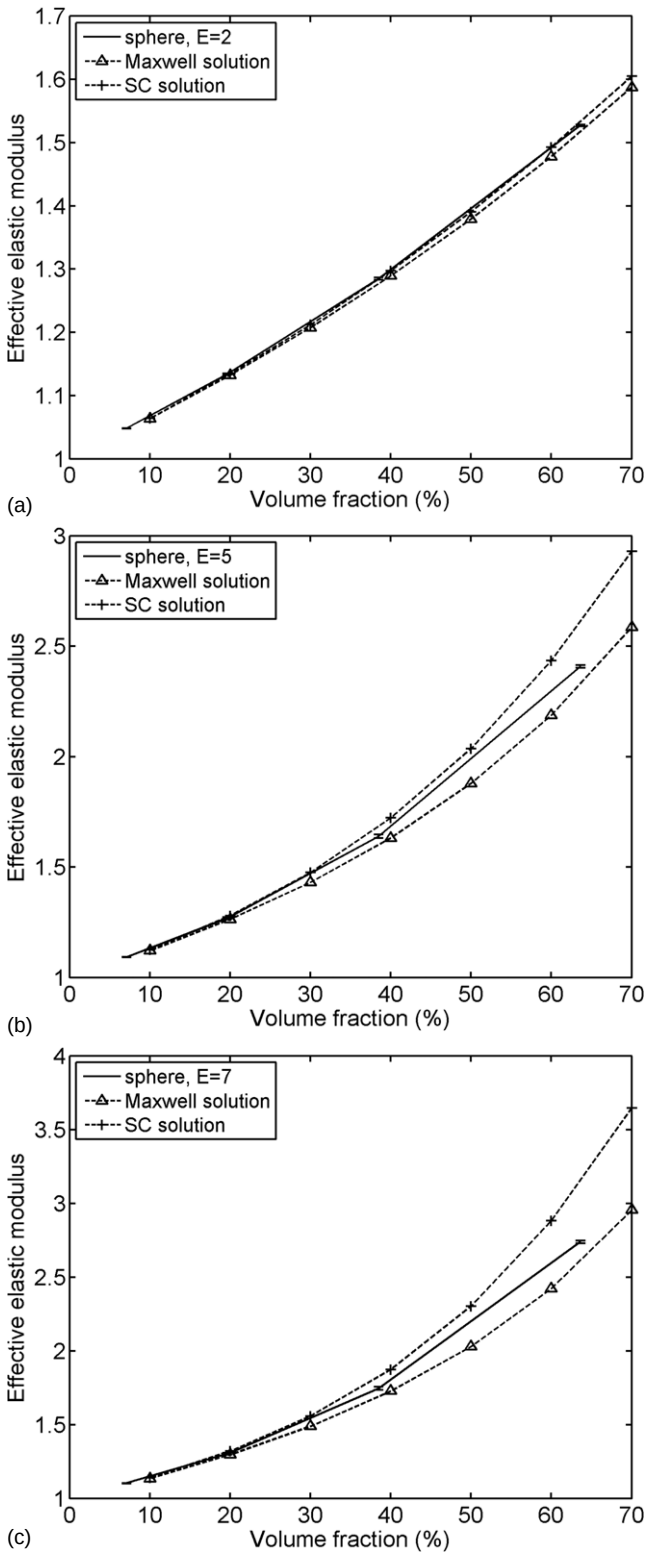

Figure 6. Comparison of normalized elastic modulus between simulations and effective medium solutions for models containing non-overlapping random circular inclusions, with (*a*) $E_2 = 2$, (*b*) $E_2 = 5$ and (*c*) $E_2 = 7$.

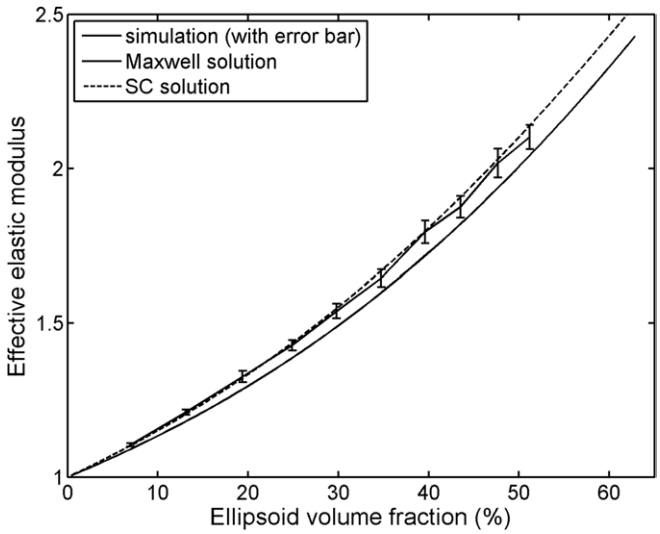

Figure 7. Comparison of normalized elastic modulus between simulations and effective medium solutions for models containing overlapping random spheres, with $E_2 = 4$.

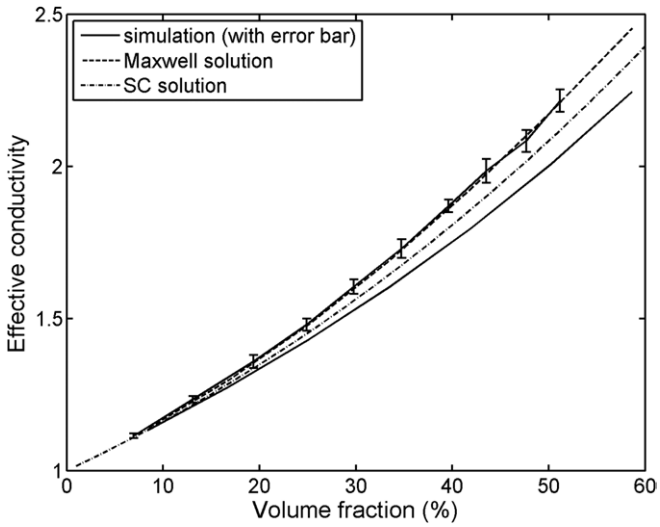

Figure 8. Comparison of normalized conductivity between simulations and effective medium solutions for models containing overlapping random spheres, with $\sigma_2 = 4$.

Maxwell approximation tends to be closer. This is somewhat different from the results of overlapping particles. Comparing figures 7 and 9(*b*), we found that the effective modulus does not differ very much between the overlapping and non-overlapping inclusions. In figure 9(*c*), E_{eff} decreases with the sphere volume fraction since the spheres are 'softer' than the matrix in this case. The comparisons between the EMTs and the simulations generally do not show satisfactory agreements here, especially at higher volume fractions. For example, when the sphere volume fraction is 50%, the finite element simulation, the Maxwell solution and the SC solution predict results of 2.3, 2.0 and 2.1, respectively. This discrepancy could be related to the limitation of the approximation theories for predicting the effective moduli of composite materials.

The corresponding conductivity analysis was also performed on non-overlapping spheres as shown in figures 10 and 11. Again, we chose the ratio of the conductivities of the matrix and the spheres to be 1 : 4 for consistency. Clearly, the simulation results fall between the SC solution and the DEM solution while the Maxwell solution underestimates the

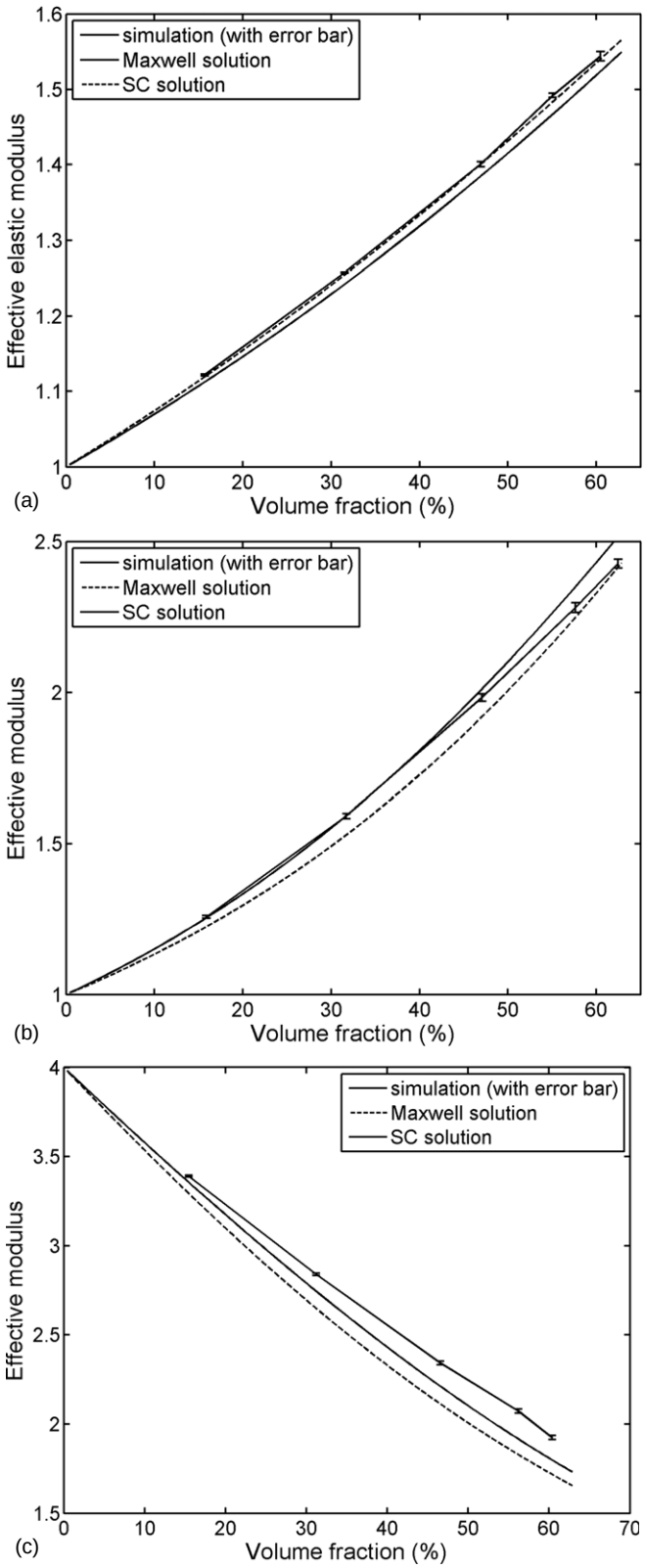

Figure 9. Comparison of normalized elastic modulus between simulations and effective medium solutions for models containing non-overlapping random spheres, with $E_2 = 4$.

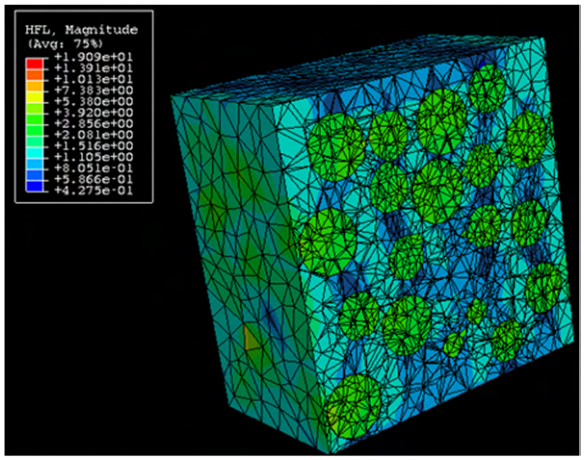

Figure 10. Finite element analysis on the conduction of non-overlapping random spheres.

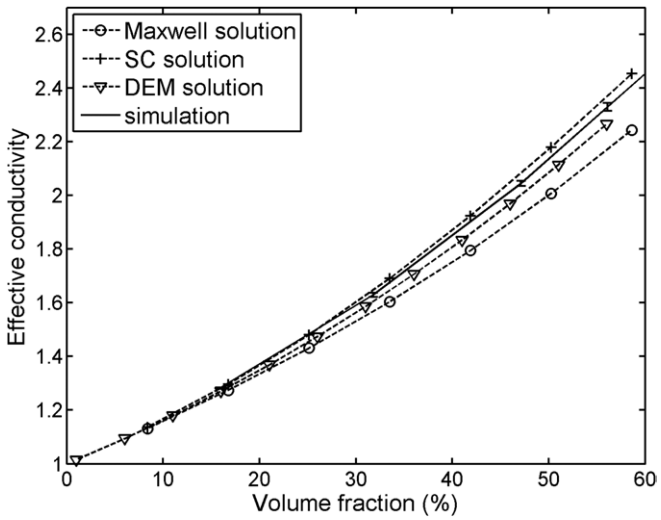

Figure 11. Comparison of normalized conductivity between simulations and effective medium solutions for models containing non-overlapping random spheres, with $\sigma_2 = 4$.

conductivity. The effective conductivity increases non-linearly as the sphere volume fraction increases. For example, at 60% volume fraction, the effective conductivity increases by approximately 150%. In addition, by comparing figures 8 and 11, we find that the conductivity does not differ very much between the overlapping and non-overlapping conditions, either.

3.3. Ellipsoidal inclusions

As mentioned previously in section 2, two types of ellipsoidal particles, namely oblate and prolate, were investigated in this work, and the outcomes of these simulations were compared with the EMTs. Figure 12 shows the mechanical analysis of a two-phase composite containing non-overlapping ellipsoidal inclusions that are either oblate or prolate. The aspect ratio for both types of ellipsoids is 1.4. Again, the correlation is excellent between the simulations and the analytical predictions. The Maxwell approximation exhibits close correlations with both types of ellipsoidal particles at

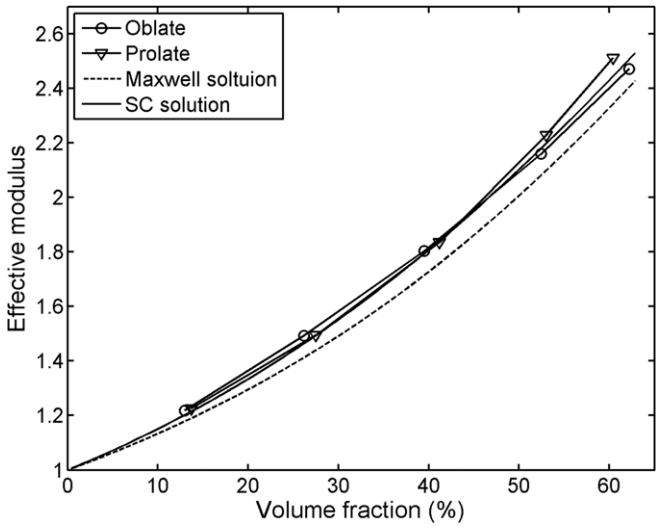

Figure 12. Comparison of normalized elastic modulus between simulations and effective medium solutions for models containing non-overlapping random ellipsoids, with $E_2 = 4$ and $\varepsilon = 1.4$.

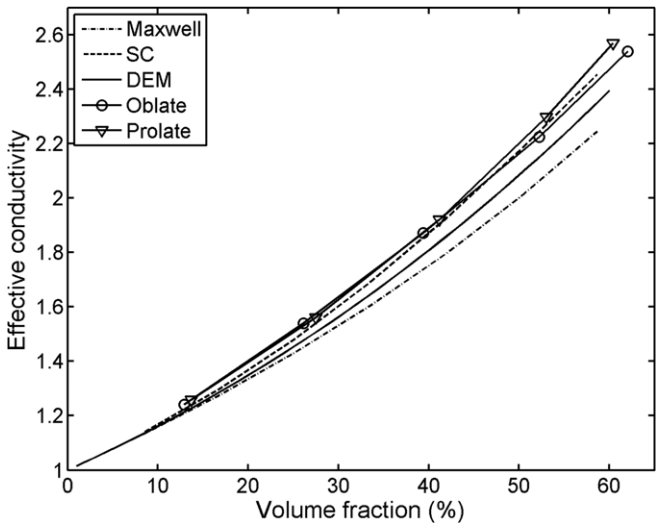

Figure 13. Comparison of normalized conductivity between simulations and effective medium solutions for models containing non-overlapping random ellipsoids, with $\sigma_2 = 4$ and $\varepsilon = 1.4$.

volume fractions below 20%. It has also been noticed that the results of the prolate and oblate particles are nearly the same at lower volume fractions, yet they start to deviate from each other at a volume fraction above 40%. This deviation increases with the volume fraction, and it is expected that at the closed-packing limit, there should be an appreciable difference between the two cases. In the conductivity analysis as shown in figure 13, it is again seen that the SC approximation provides a better prediction on the results compared with other theories. In addition, the composite containing prolate particles has a higher conductivity than that containing oblate particles, although the difference is less than 5% at a volume fraction below 60%.

The effect of aspect ratio on the effective elastic modulus is presented in figures 14(*a*) and (*b*). The 'aspect ratio', ε, is defined as the ratio of the major axis length to the minor axis length. The geometry is assumed to be a prolate ellipsoid

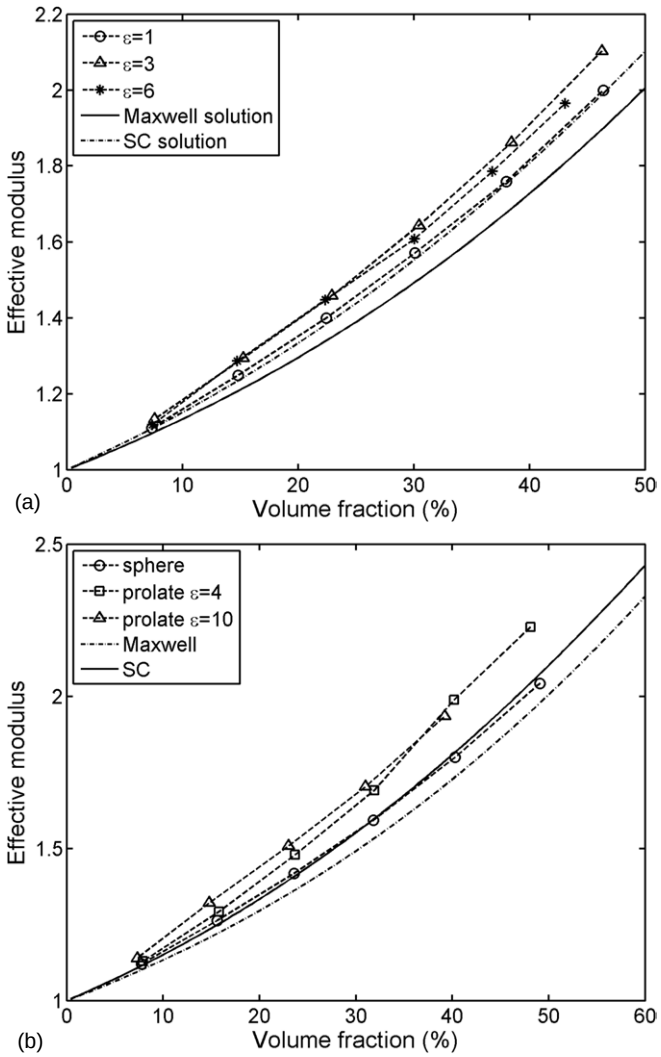

Figure 14. Effect of ellipsoid aspect ratio on effective elastic modulus: (*a*) equivalent spherical radius= 0.1; (*b*) equivalent spherical radius = 0.05.

of revolution, and hence the two minor axes have the same length. The number of ellipsoids used in the simulation varies from 170 to 1020 depending on the volume fraction of particles. From the figure, it is seen that the effective modulus of the composite is a function of the particle aspect ratio. In figure 14(*a*), the mean radius of particles is 0.1 and it is seen that the maximum modulus of ellipsoidal particle system is 5% higher than that of spheres at the same volume fraction. In figure 14(*b*) where the mean radius of particles is 0.05 and at the same volume fraction, the maximum value of the modulus is approximately 10% higher than that of a spherical particle system. Although none of the effective medium solutions agrees with the simulations, the SC approximation yields a closer result. More interestingly, evidence shows that the relationship between the modulus and the aspect ratio is not monotonic. Rather, the result oscillates when the aspect ratio varies. More specifically, the effective modulus decreases in the range $\varepsilon = 1$–2, then increases for $\varepsilon = 2$–4. The maximum value occurs at $\varepsilon = 4$ and then it decreases again. Further increase in the aspect ratio leads to only a mild change in the result: from figure 14, it can be seen that the moduli for $\varepsilon = 4$ and 10 are not far away from each other. It is conjectured that the spatial distribution of the stress concentration zones may play a role in this oscillatory result. But the exact reason behind the phenomenon is not clear yet and requires further investigation in future.

Finally, it should be pointed out that for a general two-phase elastic material system involving four distinct parameters (E_1, ν_1, E_2, ν_2), Dundurs [27] has proved that the stress field can be written in terms of only two parameters. Therefore, if Poisson's ratios of dissimilar materials are of interest, only one extra parameter needs to be included in the mechanical analysis accordingly.

4. Conclusions

In this work, a finite element modelling approach was successfully implemented to investigate the elastic modulus and conductivity of heterogeneous composites containing particulate inclusions. Both 2D and 3D models were developed and the simulation results were compared with the existing analytical approximation theories. Several important conclusions can be drawn from this study:

(1) The randomness in the particle distribution has an impact on the properties of a two-phase particulate material system. For solid inclusions, the EMTs are capable of predicting the material properties quite well, but the predictions on void inclusions are much less reliable.

(2) Among the various approximation methods, the SC solution yields much better results than the other methods including the Maxwell solution, the DEM solution and the rules of mixing. However, the SC approximation is less accurate in the following two situations: (a) particulate inclusions of large aspect ratios and (b) soft inclusion materials (i.e. the modulus of the matrix is higher than that of the inclusions).

(3) Both the effective elastic modulus and conductivity show relatively weak dependence on the permeability of the particulate inclusions—that is, at the same volume fraction, the overlapping particles and non-overlapping particles yield almost the same results.

(4) Investigation of the morphological shape of the inclusions reveals that at higher volume fractions, the prolate particles yield a higher elastic modulus and a higher conductivity than the oblate particles. However their differences are not significant.

(5) There does not exist a monotonic relationship between the properties of material containing ellipsoidal inclusions and the particle aspect ratio. The exact locations of the maxima depend on the properties of both material phases.

It should be pointed out that the 3D models and methodologies developed in this work may provide a convenient way to study mechanical and transport properties of multiphase composites for not only spherical and ellipsoidal inclusions but also short fibres as well as filler contents of other shapes.

References

[1] Hashin Z 1983 *J. Appl. Mech.* **50** 481
[2] Torquato S 1991 *Appl. Mech. Rev.* **44** 37
[3] Chen J, Xu L and Li H 2008 *Mater. Sci. Eng.* A **491** 385
[4] Hashin Z and Shtrikman S 1963 *J. Mech. Phys. Solids* **11** 127
[5] Yi Y B and Sastry A M 2004 *Proc. R. Soc. Lond.* A **460** 2353
[6] Yi Y B 2006 *Phys. Rev.* E **74** 031112
[7] Berhan L, Yi Y B, Sastry A M, Munoz E, Selvidge M and Baughman R 2004 *J. Appl. Phys.* **95** 4335
[8] Zhang T and Yi Y B 2008 *J. Appl. Phys.* **103** 014910
[9] Wang C W, Yi Y B and Sastry A M 2004 *J. Electrochem. Soc.* **151** A1489
[10] Torquato S 2002 *Random Heterogeneous Materials: Microstructure and Macroscopic Properties* (Berlin: Springer)
[11] Wei C Y, Srivastava D and Cho K 2004 *Nano Lett.* **4** 1949
[12] Maxwell J C 1873 *A Treatise on Electricity and Magnetism* (Oxford: Clarendon)
[13] Gubernatis J E and Krumhansl J A 1975 *J. Appl. Phys.* **46** 1875
[14] Mclaughlin R 1977 *Int. J. Eng. Sci.* **15** 237
[15] Mondescu R P and Muthukumar M 1999 *J. Chem. Phys.* **110** 1123
[16] Garboczi E J and Berryman J G 2001 *Mech. Mater.* **33** 455
[17] Garboczi E J and Day A R 1995 *J. Mech. Phys. Solids* **43** 1349
[18] Roberts A P and Garboczi E J 2002 *Proc. R. Soc. Lond.* A **458** 1033
[19] Cai W, Tu S and Tao G 2005 *J. Thermoplast. Compos. Mater.* **18** 241
[20] 2005 *MATLAB*® 7.1 *User's Manual* MathWorks, Inc.
[21] 2006 *COMSOL Multiphysics*® 3.3 *User's Manual* COMSOL, Inc.
[22] 2006 *ABAQUS Standard*® 6.5 *User's Manual* ABAQUS, Inc.
[23] Torquato S and Rintoul M D 1995 *Phys. Rev. Lett.* **75** 4067
[24] Miloh T and Benveniste Y 1999 *Proc. R. Soc. Lond.* A **455** 2687
[25] Benveniste Y 2006 *J. Mech. Phys. Solids* **54** 708
[26] Yi Y B 2008 *Acta Mater.* **56** 2810
[27] Dundurs J 1969 *ASME J. Appl. Mech.* **36** 650